PHILOSOPHICAL TRANSACTIONS OF THE ROYAL SOCIETY A MATHEMATICAL, PHYSICAL & ENGINEERING SCIENCES

Novel Materials for Advanced Batteries

B. C. H. Steele

Phil. Trans. R. Soc. Lond. A 1981 **302**, 361-374
doi: 10.1098/rsta.1981.0174

Phil. Trans. R. Soc. Lond. A **302**, 361–374 (1981)
Printed in Great Britain

Novel materials for advanced batteries

By B. C. H. Steele

Wolfson Unit for Solid State Ionics, Department of Metallurgy and Materials Science, Imperial College, London SW7 2AZ, U.K.

[Plate 1]

The relevance of materials science to the development of high-energy secondary batteries is discussed with reference to the complex highly defective disordered solids such as $PbO_{2-y}H_x$ and $NiOOH_x$, which are incorporated into conventional secondary battery systems. Particular emphasis, however, is given to an evaluation of the properties of novel insertion electrodes such as TiS_2 and V_6O_{13}, which exhibit high conductivities for both lithium ions and electrons. The prospects for incorporating these materials into completely solid state secondary batteries are discussed. An assessment is also given of the current status of solid lithium ion electrolytes and the behaviour of solid electrolyte/insertion electrode interfaces. A final section outlines the probable configuration of solid state batteries and emphasizes the need to optimize the properties of composite electrodes incorporating solid electrolytes and insertion electrode components.

1. Materials aspects of high-energy secondary batteries

High-energy secondary batteries are already used in electric vehicles and in association with intermittent energy sources such as wind and solar power generators. It is widely recognized (Jensen *et al.* 1979; House of Lords 1980) that improvements in battery performance are essential if this form of electrochemical energy storage is going to play a significant role in the future energy strategy of the U.K. and E.E.C. Recent surveys and conferences (Stein 1976; Libowitz & Whittingham 1979; Gross 1979; Murphy *et al.* 1980) have emphasized the importance of materials science in the development of improved and alternative secondary batteries that are required to meet the relevant operating specifications. New metallic alloys, ceramics, polymeric and composite materials are continually being fabricated and tested in the exacting environmental conditions associated with the high-energy battery systems now being developed around the world.

It is in fact a statement of the obvious that the development of batteries is essentially a material science development programme. This contention can be illustrated by selecting a few examples from the secondary battery systems summarized in table 1.

Lead–acid batteries with a much reduced maintenance requirement are rapidly becoming commonplace because of the introduction of Pb–Sb alloys with lower Sb contents and Pb–Ca–Sn alloys (May 1980). The electrochemical behaviour of these alloys reduces the amount of water lost; but initially resulted in a range of metallurgical problems associated with fabrication and loss of strength of the alloys. These problems have eventually been overcome by careful microstructural investigations. Further developments in materials technology have also made it possible to operate lead–acid batteries in a fully sealed mode by incorporating a very porous glass fibre separator, which allows oxygen evolved at the positive plate to rapidly permeate to

Table 1. Battery systems

components				current performance	
negative plate	electrolyte	positive plate	open circuit voltage/V	energy W h/kg	power W/kg
Pb	H_2SO_4 (aq)	PbO_2	2.05	30 (171)	50
Zn	KOH (aq)	NiOOH	1.7	50 (321)	150
Fe	KOH (aq)	NiOOH	1.3	60 (267)	70
Zn	$ZnCl_2$ (aq)	$Cl_2(Br_2)$	2.1	110* (465)	100
Fe	KOH (aq)	Air	1.3	81 (764)	30
Zn	KOH (aq)	Air	1.6	120* (1080)	80
Na	β-alumina (solid)	S	2.0–1.7	180* (664)	220*
Li–Al	LiCl–KCl (molten salt)	FeS	1.6	50 (870)	—
Li	organic electrolyte	TiS_2	2.4–1.9	132* (480)	—

* Projected values.

the negative, where it is recombined. The negative plate does not become further charged and no water is lost during overcharge.

Aspects of materials development in the Ni–Zn and Na–S systems have been described in other contributions to this Discussion Meeting. In contrast the prototype Li–FeS secondary battery provides an example of a system in which there appears to be no economic solution to the formidable material problems associated with the operation at 400 °C in a molten salt environment (Battles *et al.* 1978). The present technical solutions of using BN felt for the separator and Y_2O_3 cloth to retain the active electrode components are far too expensive, and alternative solutions are not apparent.

In any discussion of the materials aspects of secondary batteries, it is also important to emphasize that many of the active electrode components are complex grossly defective non-stoichiometric solids far removed from the stoichiometric molecular species usually investigated by electrochemists. Examples from batteries in current commercial production are provided by $PbO_{2-y}H_x$ and $NiOOH_x$. An understanding of the electrochemical behaviour of these and other similar non-stoichiometric oxides requires the application of a whole range of modern physical instrumental techniques. In particular it is important that as much structural information as possible be obtained so that the observations of different investigators can at least be correlated with the structure of the bulk material. In this context it should be noted that X-ray diffraction only provides an average structure over some 10^{18} unit cells, whereas many of the disordered oxide electrode materials possess a variety of local microdomain and intergrowth structures that can only be revealed by electron diffraction and imaging techniques. By using modern electron microscope instruments it is now possible, for example, to obtain electron diffraction and elemental chemical analysis from regions with diameters as small as 10 nm. This means that the composition and structure of individual electrocatalytic oxide particles can now be determined. This is illustrated in figure 1, plate 1, for the material $La_{0.7}Sr_{0.3}MnO_3$, which has been investigated as a replacement for platinum in air electrodes for batteries and fuel cells. A relatively wide electron beam will encompass many particles of the electroactive oxide powder and as these will in general be at different orientations a typical polycrystalline ring electron diffraction pattern (figure 1*a*) is obtained that is difficult to interpret. In contrast, the narrow electron beam available in modern instruments can be focused onto a single oxide particle and the corresponding single crystal electron diffraction pattern (figure 1*b*) is much more amenable to interpretation. In addition an elemental chemical analysis can be made of

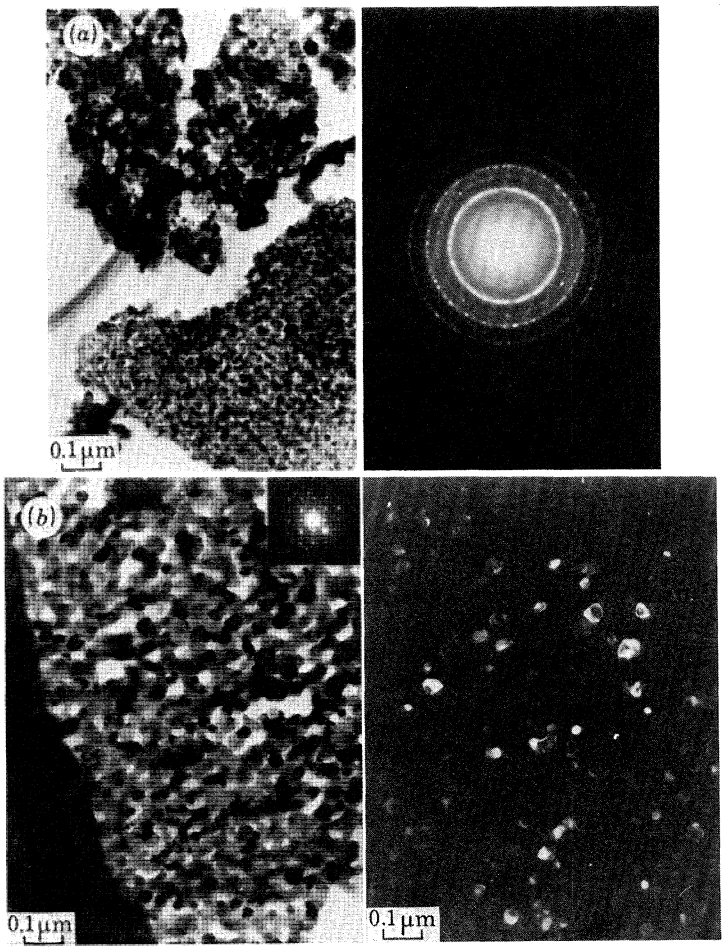

FIGURE 1. (*a*) Transmission electron micrograph of polycrystalline aggregate of $La_{0.7}Sr_{0.3}MnO_{3-x}$ electrocatalyst. The broad electron beam produces a polycrystalline ring diffraction pattern. (*b*) Transmission electron micrography (bright field image) of polycrystalline aggregate of $La_{0.7}Sr_{0.3}MnO_{3-x}$ electrocatalysts (left). Narrow electron beam enables single crystal diffraction spots to be obtained from small (*ca.* 50 nm) particles shown in dark field image (right).

(*Facing p.* 362)

PHILOSOPHICAL TRANSACTIONS OF THE ROYAL SOCIETY A MATHEMATICAL, PHYSICAL & ENGINEERING SCIENCES

the individual oxide particles (Hadjicostantis 1978). The presence of local intergrowth structures in a complex oxide $LaNiO_{3-x}$, which has been proposed as another air electrode material is also revealed by high-resolution electron microscopy (J. Drennan, personal communication, 1980). It is known (Trasatti (ed.) 1980) that electronic and mass transport properties together with the surface reactivity oxide electrodes are strongly influenced by the composition and structure of the bulk material. These and other structural features must be characterized if progress is to be made in elucidating the behaviour of complex non-stoichiometric electrode materials, and in ameliorating the present situation in which conflicting observations on the electrochemical performance of poorly characterized materials are continually published in the literature.

2. Insertion electrode materials

2.1. *General comments*

All the systems in table 1, except for Li/TiS_2, may be regarded as essentially classical secondary battery systems in that the charge–discharge reaction involves the formation of new phases. Nucleation and growth of these new phases often restricts the magnitude of the current and power density. The associated morphological changes can also lead to a loss of active electrode material and consequent deterioration in overall performances. In contrast, the alternative concept of insertion electrode materials avoids the formation of new phases and also overcomes many of the problems associated with the construction of completely solid state batteries.

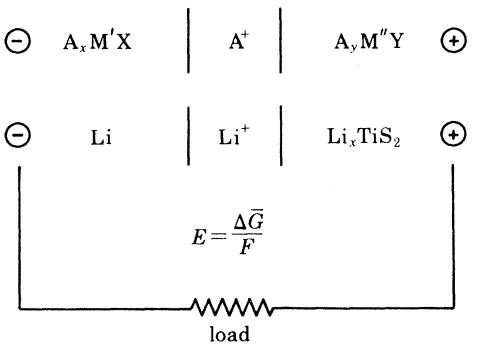

Figure 2. Mode of operation of cell incorporating insertion electrode Li_xTiS_2.

The concept of using insertion or solid solution electrodes in high energy secondary batteries was first discussed by Steele (1973) and Armand (1973). The mode of operation of these electrode materials can be explained with reference to figure 2, using TiS_2 as a specific example. During the discharge reaction, lithium ions are produced at the negative plate electrode. These ions migrate across the electrolyte phase and are then inserted into the TiS_2 host lattice thus producing the solid solution Li_xTiS_2. At the same time an equal number of electrons are transported around the external circuit and are incorporated into the Li_xTiS_2 insertion electrode. The discharge process thus consists of a double injection of ions and electrons into the TiS_2 host lattice and does not involve the formation of a new phase. It should be noted that the limiting composition of the Li_xTiS_2 phase at room temperature appears to have a value of x around 1.6, although the e.m.f. associated with the additional 0.6 g atom of lithium is too low to be exploited in a high-energy density battery. The absence of high resistive reaction products at the electro-

lyte–electrode interface obviously facilitates the design of completely solid state batteries. To ensure that the cell can be discharged at a high current density it is essential that the insertion electrode exhibits both a high ionic and electronic conductivity. The solid insertion electrode thus functions as a mixed conductor. It is also possible to insert Li^+ ions into TiS_2 chemically by using solutions of *n*-butyllithium dissolved in hexane. Using this technique Chianelli (1976), for example, has been able to observe directly in an optical microscope the insertion of Li^+ ions into single crystal TiS_2. As well as confirming that the single crystal remained intact he was also able to study the kinetics of the lithium insertion.

Other desirable properties include a large range of stoichiometry to ensure a high capacity for the electroactive species, and an appropriate open-circuit voltage that does not change too rapidly with composition. These properties are essentially controlled by the thermodynamic behaviour of the insertion electrode material, and the principal features influencing this behaviour are discussed in the next section. For the specific example of Li_xTiS_2 ($0 < x < 1$) these thermodynamic features result in the theoretical specific energy density of 480 W h/kg, which compares well with values for other advanced battery systems listed in table 1. For technological applications it is also important that the insertion electrode be stable in contact with the electrolyte and also be able to be fabricated economically.

Finally it should be noted that the negative plate electrode could also be an appropriate insertion electrode material (A_x M′Y), thus making possible a cell incorporating two different insertion electrodes as depicted in figure 2.

2.2 *Thermodynamic and transport properties of* Li_xTiS_2

The open circuit voltage (e.m.f.) at 298 K of the cell,

$$Li|Li^+|Li_xTiS_2,$$

is reproduced in figure 3 and provides a measurement of the partial molar free energy of solution of lithium ($\Delta\bar{G}_{Li}$) in TiS_2 according to the equation

$$\Delta\bar{G} = -nEF.$$

The associated partial molar enthalpy ($\Delta\bar{H}_{Li}$) and entropy ($\Delta\bar{S}_{Li}$) terms are also related by the expression

$$\Delta\bar{G} = \Delta\bar{H} - T\Delta\bar{S}.$$

The shape of the e.m.f. curve as a function of composition is thus determined by the variation of $\Delta\bar{H}_{Li}$ and $\Delta\bar{S}_{Li}$ as a function of x in Li_xTiS_2. These enthalpy and entropy terms must also reflect the separate contributions (Cheung *et al.* 1979) arising from the double injection of lithium ions and electrons into the TiS_2 lattice according to the equation

$$x\,Li \rightarrow x\,\{Li^+_{TiS_2} + e^-_{TiS_2}\} \rightarrow Li_xTiS_2.$$

The following simple relation can reproduce the principal features of the Li_xTiS_2 e.m.f. curve:

$$\Delta\bar{G} = \Delta E_1 + x\,\Delta E_2 + RT\ln\{x/(1-x)\}.$$

It can also provide some general observations about the thermodynamic properties of other insertion electrodes. To a first approximation, ΔE_1 is independent of composition and represents the energy change associated with inserting the electron into the appropriate available electronic state in TiS_2. This is believed (Whittingham 1978) to be a t_{2g} level produced by the crystal field splitting of the titanium d orbitals in the octahedral environment of the surrounding sulphur ions. The energetics of the electronic level occupied by the inserted electron determines the

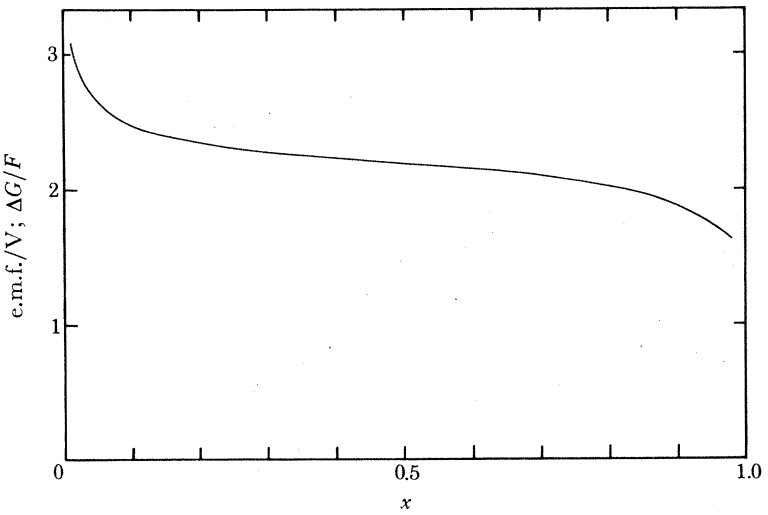

FIGURE 3. E.m.f. values at 298 K with respect to pure lithium for insertion electrode Li_xTiS_2. Theoretical specific energy density is 450 W h/kg.

overall magnitude of the e.m.f. measured. For example, if the injected electrons occupy a low-lying electronic level in the host lattice, the insertion electrode is functioning as a highly oxidizing phase and a large cell e.m.f. with respect to pure lithium metal will be developed. The other terms are responsible for the relatively smaller e.m.f. variations with composition. The distribution of the lithium ions over the available octahedral sites in the Van der Waals layer in TiS_2 (see figure 4) is responsible for the configuration entropy term $RT \ln \{x/(1-x)\}$, and electrostatic interactions between the inserted lithium ions will introduce a relatively small composition-dependent enthalpy term ($x\ \Delta E_2$). It is also possible that the filling of the electronic states will make a contribution to the composition-dependent enthalpy term ($x\ \Delta E_2$) when the electrons are being accommodated within a wide band. Electronic contributions to the configurational entropy and changes in the vibrational entropy have been omitted from the simple expression, which does, however, have the merit of being able to reproduce the general features of the e.m.f.–composition curves observed for many insertion compounds. It follows that the compositional limit for a particular insertion electrode will be determined by either the number of available lattice sites in the host electrode material or the number of electronic states in the relevant band. If sufficient lattice sites are available it is possible for the inserted electrons to start filling the next available band, but this process would be accompanied by a sharp transition in the e.m.f.–composition curve.

The ionic transport properties of Li_xTiS_2 can best be discussed with reference to figure 4, which contains a schematic representation of the crystallographic structure of TiS_2. Layers of TiS_2 are held together by Van der Waals forces, and the inserted lithium ions occupy sites within the Van der Waal gap. The insertion of the lithium ions is accompanied by an expansion of the unit cell in the c direction by about 9 %. This lattice expansion together with Knight shift and n.m.r. measurements indicate that the lithium is present as lithium ions sandwiched between negatively charged TiS_2 layers containing itinerant electrons that are not localized on the Ti^{4+} ions. It is believed that the Li^+ ions predominantly occupy the octahedral sites within the Van der Waals layer, and as there are twice as many empty tetrahedral sites a low energy

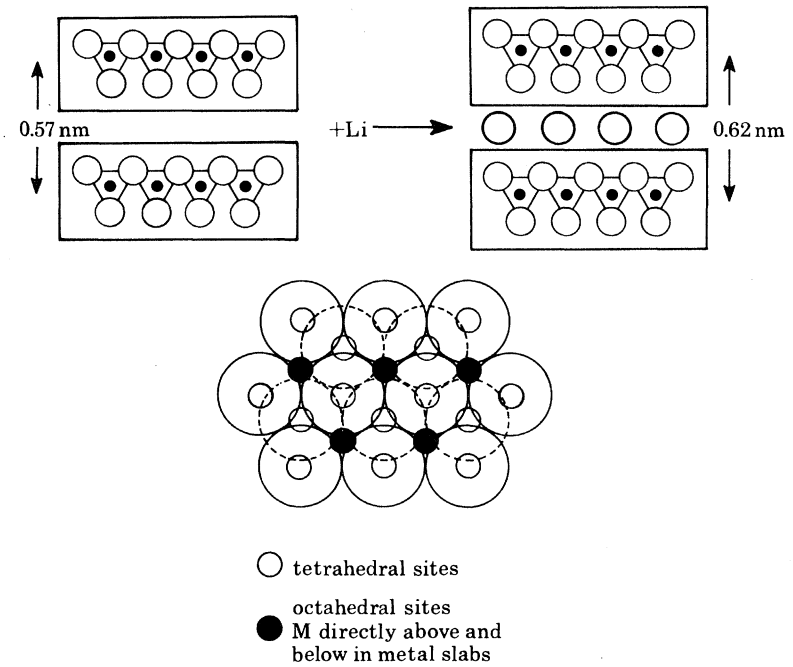

FIGURE 4. Representation of lithium insertion into the Van der Waals layer of a TiS_2 crystal, producing lattice expansion in the c direction. The lithium ions occupy the octahedral sites within the layer as shown in the lower diagram.

diffusion path, involving jumps between octahedral, tetrahedral and octahedral sites, is thus available to a diffusing lithium ion. The activation energy (0.1 eV) for self-diffusion (D^*) derived from n.m.r. measurements (Berthier 1979) is indicative of a facile diffusion process. Chemical diffusion coefficients ($\tilde{D}$) derived from potentiostatic and galvanostatic pulse experiments (Winn *et al.* 1976; Basu & Worrell 1979) are in the range 10^{-8} to 10^{-9} cm^2/s at room temperature, and these values are about an order of magnitude greater than the n.m.r. self-diffusion (D^*) values in accordance with the relation

$$\tilde{D} = D^* \, (\mathrm{d} \ln a)/(\mathrm{d} \ln X),$$

where the thermodynamic factor, $(\mathrm{d} \ln a)/(\mathrm{d} \ln X)$, takes account of the variation of the activity (a) of the diffusing species with mole fraction (X).

Owing to the ready availability of vacant tetrahedral sites, the diffusion coefficients show only a small dependence upon the lithium content of $Li_xTi_{1+y}S_2$. However, the presence of excess titanium ($y > 0$) in the host lattice has a very significant effect upon the lithium diffusion rate. The additional titanium ions are accommodated within the Van der Waals gap and not only occupy the same sites as the inserted lithium ions but are responsible for much stronger bonding between the adjacent TiS_2 layers, which in turn makes lithium transport that much more difficult.

When powders of TiS_2 with a diameter less than 20 μm and possessing a lithium diffusion coefficient of 10^{-8} cm^2/s are incorporated into a porous electrode, calculations have suggested (Atlung *et al.* 1979) that such an electrode should be able to sustain current densities of around 10 mA/cm^2. Experimental values reported by Whittingham (1976) are in accordance with this

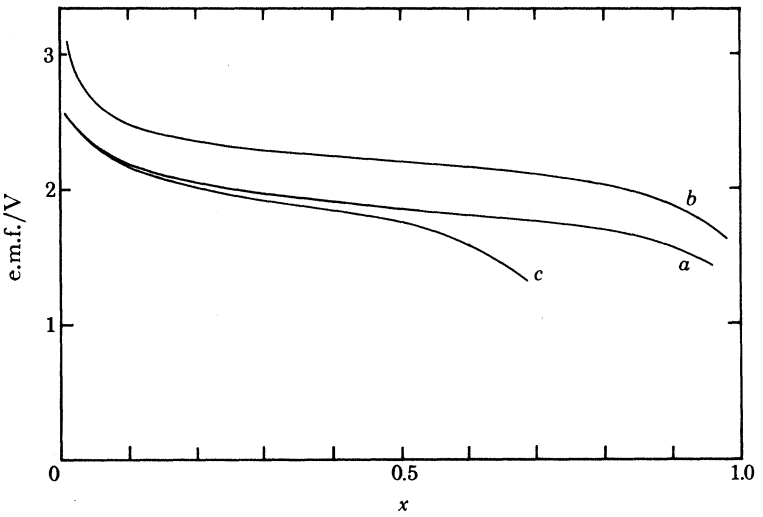

FIGURE 5. Dynamic behaviour of Li_xTiS_2 insertion electrodes subjected to charge–discharge cycles. Conditions: $\tilde{D} > 10^{-8}$ cm²/s; size less than 20 μm; $i \approx 10$ mA/cm². (*a*) Initial; (*b*) open circuit e.m.f. for single crystal of $Ti_{1+y}S_2$; (*c*) 1000 cycles at 70 % theoretical capacity, galvanostatic experiments at 10 mA/cm².

conclusion and are reproduced in figure 5. A feature of this investigation was the high degree of reversibility exhibited by the TiS_2 particles and the retention of much of the capacity even after 1000 cycles. The very satisfactory performance of TiS_2 electrodes in these experiments encouraged the Exxon laboratories to carry out further tests on larger prototype batteries. These investigations (Gaines *et al.* 1976) revealed that the organic electrolyte employed, dioxolane incorporating $LiClO_4$, could be explosive under certain operating conditions. This particular electrolyte had been selected because of its high ionic conductivity and other features associated with the behaviour of the Li–Al negative plate electrode. In spite of further extensive investigations, a satisfactory alternative to the dioxolane–$LiClO_4$ organic electrolyte has not been developed (Rao *et al.* 1980), and most development programmes now envisage using TiS_2 electrodes with either a molten salt or solid electrolyte (§4). It should be emphasized, however, that the performance of the TiS_2 material was entirely satisfactory and in accordance with the specifications required for operation in electric vehicle batteries (Gaines *et al.* 1976).

2.3. *Alternative insertion electrode materials*

Although TiS_2 has many desirable features, a variety of alternative electrode materials have also been investigated to determine whether they offer any advantages over TiS_2. A selection of these electrode materials is shown in figure 6, which depicts the potential range associated with the lithium insertion reaction. A more extensive summary is given by Trumbore (1979). The mass transport properties of these electrodes have been determined by standard galvanostatic or potentiostatic methods, and occasionally more detailed investigations have been made with the use of an eight-point conductivity technique described by Dudley & Steele (1980). Attention is drawn to the high potentials exhibited by CoO_2 and NiO_2 (Mizushima *et al.* 1980), which can be attributed to the very oxidizing environment created by the presence of Co^{4+} and Ni^{4+} ions. These oxides can reversibly incorporate almost 1 g atom of lithium and the associated theoretical specific energy density is in excess of 1000 W h/kg. The insertion compound V_6O_{13}

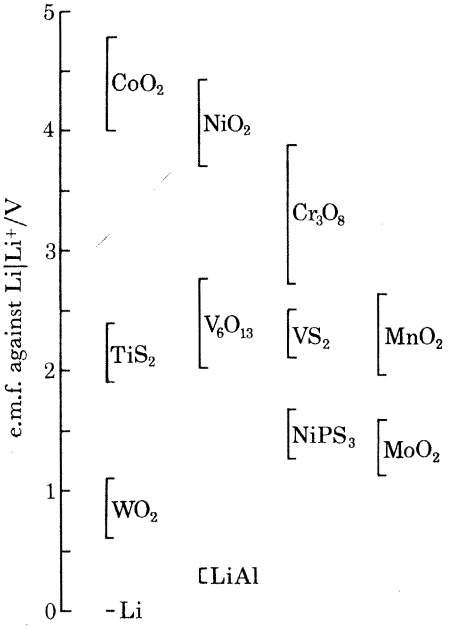

FIGURE 6. Potential range of selected insertion electrode materials.

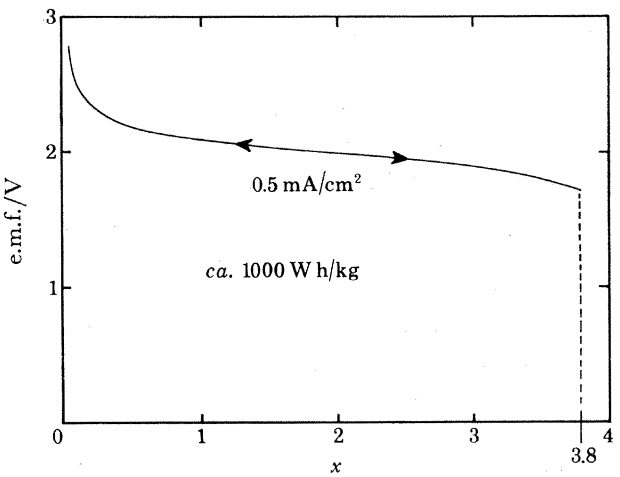

FIGURE 7. E.m.f. values with respect to lithium for amorphous insertion electrode Li_xMoS_3.

also possesses a useful theoretical specific energy density value of about 800 W h/kg (Murphy *et al.* 1979). Moreover, the lithium ions are accommodated in the intersecting channels of a three-dimensional framework structure formed by arrays of corner and edge-shared VO_6 octahedra. A high proportion of the lithium ions can be inserted with only a small volume change, which could be a significant advantage when incorporating V_6O_{13} into a completely solid state battery. It is also known that the hyperstoichiometric material $V_6O_{13.2}$ exhibits superior lithium mass transport behaviour. Lattice images (J. M. Thomas & D. Patterson, private communication, 1980) obtained by high-resolution electron microscopy of non-stoichiometric material prepared in the Wolfson Unit for Solid State Ionics reveal a complicated structure incorporating a variety of extended defects and intergrowth regions. This type of

disorder can only be examined by electron microscopy and provides a further example of the importance of physical instrumental techniques in understanding the thermodynamic and transport behaviour of grossly defective non-stoichiometric electrode materials.

An extreme example of a disordered insertion compound is provided by amorphous MoS_3, which can be prepared by the decomposition of ammonium thiomolybdate. When used as a positive plate electrode this material can reversibly incorporate up to 3.8 g atoms of lithium (Jacobson 1979) at an average potential of 1.9 V, which is equivalent to a theoretical specific energy of approximately 1000 W h/kg. The associated potential–composition curve is reproduced in figure 7. It can be seen from the preceding remarks that many materials are now available that satisfy the requirements for a positive plate insertion electrode. The situation for the negative electrode, however, is not so satisfactory. Most investigators are using elemental lithium, or compositions in the Li–Al and Li–Si systems (Rao *et al.* 1977; Liang *et al.* 1978), but there is little information about the performance of electrodes incorporating these materials after extended periods of charge–discharge cycling. It may be necessary to develop alternative insertion intermetallic alloys with lithium capacity and transport properties comparable with the many compounds now available for use as positive insertion electrode materials.

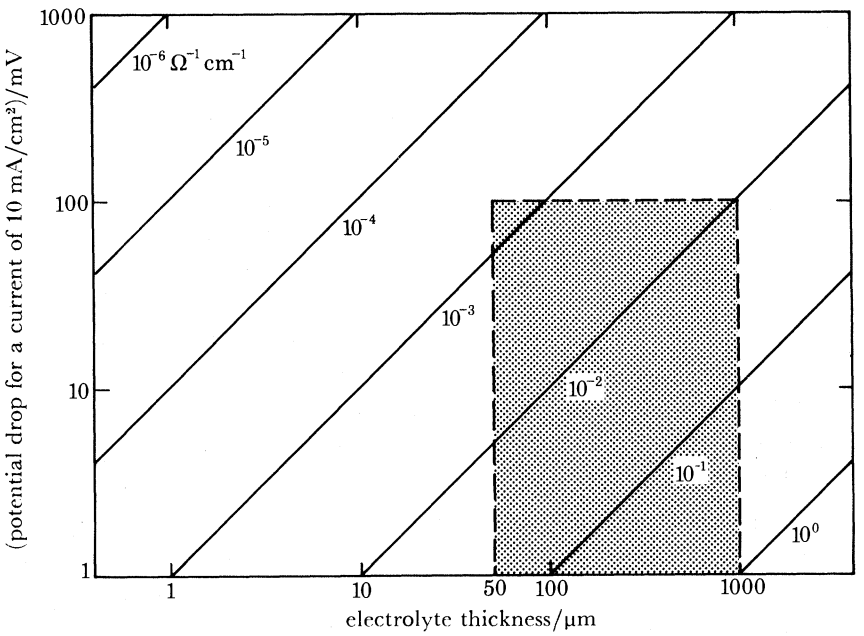

FIGURE 8. Potential drop for a current density of 10 mA/cm² as a function of electrolyte thickness for selected specific conductivity values. The shaded area indicates region of probable technological interest.

3. SOLID LITHIUM ION ELECTROLYTES

The availability of lithium insertion electrode materials makes it probable that prototype high-energy secondary solid state batteries will incorporate solid lithium ion electrolytes. It is therefore appropriate to examine the present situation with regard to these electrolytes. The basic requirements for a solid electrolyte to be incorporated into a battery can be discussed with reference to figure 8, which depicts the voltage (*IR*) developed across electrolytes as a function

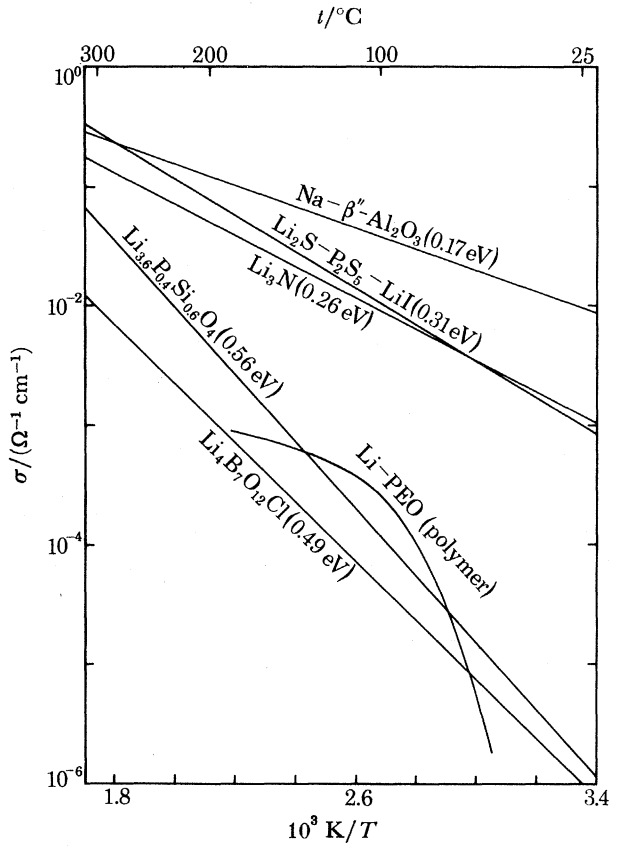

FIGURE 9. Specific conductivity values of selected lithium ion solid electrolytes as a function of reciprocal temperature. Activation energy values are given in parentheses.

of specific conductivity and thickness for a current density of 10 mA/cm². If we assume that the maximum *IR* voltage loss that can be tolerated is 100 mV and the minimum practical thickness likely to be achieved is 50 μm, then it can be concluded that the specific conductivity must exceed 10^{-3} Ω^{-1} cm^{-1}. In fact the most probable operating specifications will be within the shaded area shown in figure 8. The attainment of higher specific conductivity values is accompanied by a relaxation in the acceptable maximum electrolyte thickness. The properties of selected solid lithium ion electrolytes are summarized in figure 9, which also incorporates data for the Na–β″-Al_2O_3 electrolyte (Collongues *et al.* 1979) used in the Na–S cell (table 1). The first point to emphasize is that the specific conductivity values for all the lithium ion conductors are below the value reported for Na–β″-Al_2O_3. Although this latter electrolyte is a two-dimensional framework conductor, alternative three-dimensional framework sodium ion conductors have been successfully synthesized (Goodenough *et al.* 1976; Shannon *et al.* 1978) with comparable properties, and it can be concluded that useful sodium ion conductors have been successfully developed by using 'lattice engineering' concepts. In contrast, the synthesis of superionic crystalline lithium ion electrolytes has been much more difficult. Data for two of the better electrolytes, $Li_4B_7O_{12}Cl$, and $Li_{3.6}O_{0.4}Si_{0.6}O_4$ are shown in figure 9, and the relatively high value of about 0.5 eV (cf. 0.18 eV for Na–β″-Al_2O_3) for the activation energy for lithium ion migration in these materials means that specific conductivity values greater than 10^{-3} Ω^{-1} cm^{-1} are only attained at relatively high temperatures, in excess of 200 °C. It was con-

sidered that migration of the small lithium ion would be faciliated by the presence of the highly polarizable N^{3-} ion, and accordingly von Alpen *et al.* (1977) investigated the properties of Li_3N. As shown in figure 9, the lithium ion conductivity in Li_3N is indeed sufficiently high to satisfy the requirements for the electrolyte phase in a solid state battery. Unfortunately, however, Li_3N possesses a relatively low thermodynamic decomposition potential (0.44 V at room temperature), which must raise serious doubts about the long-term stability of this material when exposed to the exacting environmental conditions associated with secondary high-energy batteries. The development of non-crystalline lithium ion conductors has met with more success. The lithium ion transport properties of a sulphide glass, Li_2S–P_2S_5–LiI, are reproduced in figure 9. It has been reported (Malugani & Robert 1980) that the stability of this material also exceeds 2 V, which will ensure that this and other similar glasses will be extensively investigated as promising electrolyte components in an all solid state battery.

Information is also contained in figure 9 relating to a typical polymeric lithium ion electrolyte. Polymeric ethylene oxide (PEO) and propylene oxide (PPO) incorporating appropriate lithium salts were first developed as solid lithium ion conductors by Armand *et al.* (1979). Although they are relatively poor conductors at room temperature, the specific conductivity can attain values around $10^{-3}\ \Omega^{-1}\ cm^{-1}$ at 120 °C. These polymeric electrolytes can easily be fabricated into thin films, and certain of the formulations also exhibit elastomeric properties, which could be very desirable in the construction of completely solid state batteries. Moreover, initial experiments have indicated that PEO electrolytes are kinetically stable in contact with both elemental lithium and TiS_2 electrodes up to temperatures of 140 °C, provided that the polymers are anhydrous. Investigations are now in progress around the world to optimize the composition of these interesting novel polymeric electrolytes and to understand the details of the mechanism of lithium ion transport.

Although not featured in figure 9, composite electrolytes of the type LiI–Al_2O_3 should also be mentioned, as they have properties (Liang *et al.* 1978) comparable with the crystalline lithium ion electrolytes (e.g. $Li_4B_7O_{12}Cl$). Although explanations for the mechanism of enhanced lithium ion transport in these composite electrolytes remain controversial, there is still widespread interest in these materials as possible electrolytes in solid state batteries.

It can be concluded that there are now available a few solid lithium ion electrolytes that could be incorporated into solid state batteries designed to produce current densities up to 10 mA/cm². It should be emphasized, however, that such batteries would have to be operated in the temperature range 100–150 °C and that the desirable goal of ambient temperature operation is not feasible at present owing to the absence of a lithium ion electrolyte with the required specific conductivity.

4. Interfacial considerations

It is obviously difficult to fabricate good solid electrolyte–electrode interfacial contacts capable of withstanding the stresses generated during repeated charge–discharge cycles. Experience within the Wolfson Unit for Solid State Ionics has indicated that it is possible to fabricate appropriate solid–solid interfaces provided that at least one of the components can exhibit some degree of either elastic or plastic deformation. This can often be achieved at moderate temperatures (25–150 °C) with selected inorganic electrolytes, for example, Ag_2WO_4.AgI (Bonino *et al.* 1980), 47CuBr.3$(CH_3)_2$ $C_6H_{12}N_2Br_2$ (Shemilt *et al.* 1981) and LiI–Al_2O_3

PHILOSOPHICAL TRANSACTIONS OF THE ROYAL SOCIETY A MATHEMATICAL, PHYSICAL & ENGINEERING SCIENCES

(Liang *et al.* 1978). Alternatively the polymeric electrolyte mentioned in the previous section can be used to maintain the integrity of solid electrolyte–electrode interfaces.

Measurements on well designed solid–solid interfaces (Cheung *et al.* 1979; Owen *et al.* 1981) indicate that the interfacial impedance can be very small indeed, which implies that the energy barriers to ion transfer are also small. This observation introduces some interesting theoretical implications relating to the entire concept of insertion electrode materials, which function by dissolving the relevant electroactive ionic species. The classical Faraday reaction involving electron transfer at a well defined electrolyte–electrode interface is replaced by a more diffuse process involving the double injection of an ion and an electron into the host lattice over an extended region of space. It is not apparent, for example, that the electrode kinetics are best described by the conventional Butler–Volmer equation, and a recent model proposed by Beni (1980) might be more appropriate; he has developed the small polaron theory to describe the motion of an ion between adjacent sites in response to fluctuations in the dielectric properties of the surrounding medium that are associated with ion transfer across a solid electrolyte – insertion electrode interface. Whatever theoretical approaches are used to describe the transfer of ions across solid electrolyte–electrode interfaces, it should be emphasized that it does appear possible to fabricate interfaces that can satisfy the technological requirements for solid state batteries.

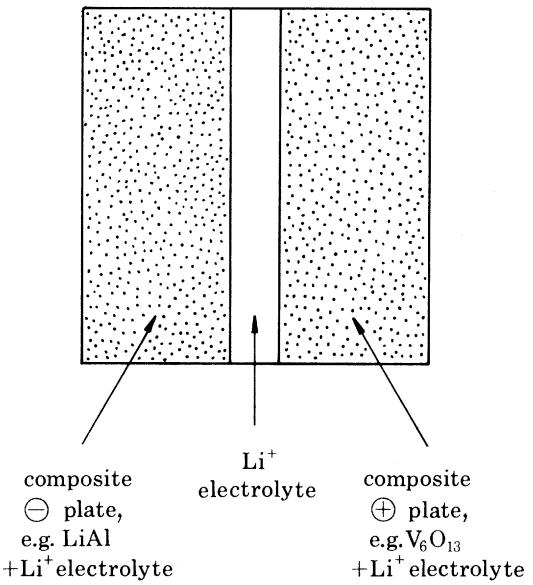

FIGURE 10. Schematic diagram of solid state cell with composite electrodes incorporating insertion electrodes.

5. CONCLUDING REMARKS

It has been suggested in the preceding sections that the properties of lithium insertion electrodes and solid lithium ion electrolytes as individual components should be able to perform satisfactorily in solid state high-energy secondary batteries. Such systems are now being constructed and will be subjected to extensive tests to examine whether the combined cell assembly can achieve the performance expected from the available information on the behaviour of the individual components. The most probable cell configuration is depicted in figure 10, in which

PHILOSOPHICAL TRANSACTIONS OF THE ROYAL SOCIETY A MATHEMATICAL, PHYSICAL & ENGINEERING SCIENCES

the composite electrodes represent the solid state analogue of the porous electrodes incorporated into cells using liquid electrolytes. Little is known about the properties of such composite electrodes, and the relative contributions made by the solid electrolyte and electrode phases to mass transport need to be carefully analysed so that the relevant material specifications can be defined. A preliminary evaluation by Owen (1981) of a composite electrode containing a high volume fraction of insertion electrode component confirms that the transport properties of the electrolyte phase are the most critical parameters and regulate the maximum current that can be drawn from the composite electrode. The effect of any volume changes during repeated charge–discharge cycles needs to be monitored with particular emphasis upon the integrity of the solid electrolyte – electrode interface. It is expected that progress in the next 2–3 years will determine whether solid state batteries can achieve a technological breakthrough or will be confined to relatively small-scale applications requiring the special features of solid state devices. It is also probable that future projects will investigate the feasibility of devising insertion electrodes able to accommodate sodium ions instead of lithium ions.

Finally it should be noted that the introduction of the concept of insertion electrodes has stimulated a re-examination of classical battery electrodes such as $NiOOH_x$ and $PbO_{2-y}H_x$ (Rickert 1980), which also function in part at least as insertion electrodes with a marked topochemical relation between the initial and final states.

I wish to acknowledge the help received from other members of the Wolfson Unit for Solid State Ionics whose investigations and comments have assisted in the preparation of this brief review.

References (Steele)

Armand, M. B. 1973 In *Fast ion transport in solids* (ed. W. Van Gool), pp. 665–673. North-Holland.
Armand, M. B., Chabagno, J. M. & Duclot, M. J. 1979 In *Fast ion transport in solids* (ed. P. Vashishta, J. N. Mundy & G. K. Shenoy), pp. 131–136. North-Holland.
Atlung, S., West, K. & Jocobsen, T. 1979 *J. electrochem. Soc.* **126**, 1311–1321.
Basu, S. & Worrell, W. L. 1979 In *Fast ion transport in solids* (ed. P. Vashishta, J. N. Mundy & G. K. Shenoy), pp. 149–152. North-Holland.
Battles, J. E., Smaga, J. A. & Myles, K. M. 1978 *Metall. Trans.* A **9**, 183–191.
Beni, G. 1980 *J. electrochem. Soc.* **127**, 467C–477C.
Berthier, C. 1979 In *Fast ion transport in solids* (ed. P. Vashishta, J. N. Mundy & G. K. Shenoy), pp. 171–176. North-Holland.
Bonino, F., Lazzari, M., Vincent, C. A. & Wandless, A. R. 1980 *Solid State Ionics* **1**, 311–318.
Cheung, K. Y., Steele, B. C. H. & Dudley, G. J. 1979 In *Fast ion transport in solids* (ed. P. Vashishta, J. N. Mundy & G. K. Shenoy), pp. 141–148. North-Holland.
Chianelli, R. R. 1976 *J. Cryst. Growth* **34**, 239–244.
Collongues, R., Kahn, A. & Michel, D. 1979 *A. Rev. Mater. Sci.* **9**, 123–150.
Dudley, G. J. & Steele, B. C. H. 1980 *J. solid State Chem.* **31**, 233–247.
Gaines, L. H., Francie, R. W., Newman, G. H. & Rao, B. M. L. 1976 In *Proc. 11th I.E.C.E.C.*, pp. 476–483.
Goodenough, J. B., Hong, H. Y. P. & Kafalas, J. A. 1976 *Mater. Res. Bull.* **11**, 203–220.
Gross, S. 1979 *Battery design and optimisation*. New Jersey: Electrochemical Society.
Hadjicostantis, D. 1978 Ph.D. thesis, University of London.
House of Lords 1980 *First Report of Select Committee on Science and Technology: Electric Vehicles*. London: H.M.S.O.
Jacobson, A. J., Chianelli, R. R., Rich, S. M. & Whittingham, M. S. 1979 *Mater. Res. Bull.* **14**, 1437–1448.
Jensen, J., McGeehin, P. & Dell, R. 1979 *Electric batteries for energy storage and conservation*. Odense University Press.
Liang, C. C., Joshi, A. V. & Hamilton, N. E. 1978 *J. appl. Electrochem.* **8**, 445–454.
Libowitz, G. G. & Whittingham, M. S. 1979 *Materials science in energy technology*. Academic Press.
Malugani, J. P. & Robert, G. 1980 *Solid State Ionics* **1**, 519–523.
May, G. J. 1980 *Metallurgist Mater. Technologist*, pp. 546–548.
Mizushima, K., Jones, P. C., Wiseman, P. J. & Goodenough, J. B. 1980 *Mater. Res. Bull.* **15**, 783–789.
Murphy, D. W., Broadhead, J. & Steele, B. C. H. 1980 *Materials for advanced batteries*. Plenum Press.

PHILOSOPHICAL TRANSACTIONS OF THE ROYAL SOCIETY A MATHEMATICAL, PHYSICAL & ENGINEERING SCIENCES

Murphy, D. W., Christian, P. A., De Salvo, F. J. & Carides, J. N. 1979 *J. electrochem. Soc.* **126**, 497–499.
Owen, J. R. 1981 In *Proc. of Twelfth International Power Sources Symposium.* (In the press.)
Owen, J. R., Lloyd-Williams, S. C., Lagos, G., Spurdens, P. C. & Steele, B. C. H. 1981 In *Proc. Int. Conf. on Lithium Batteries*, Case Western Institute of Technology, June 1980. (In the press.)
Rao, B. M. L., Eustace, D. J. & Shropshire, J. A. 1980 *J. appl. Electrochem.* **10**, 757–763.
Rao, B. M. L., Francis, R. W. & Christopher, H. A. 1977 *J. electrochem. Soc.* **124**, 1490–1492.
Rickert, H. 1980 In *Electrodes of conductive metallic oxides* (ed. S. Trasatti), pp. 183–220. Elsevier.
Shannon, R. D., Taylor, B. E., Gier, T. E., Chen, H.-Y. & Berzins, T. 1978 *Inorg. Chem.* **17**, 958–964.
Shemilt, J. M., Steele, B. C. H. & Weston, J. E. 1981 *Solid State Ionics* **2**. (In the press.)
Steele, B. C. H. 1973 In *Fast ion transport in solids* (ed. W. Van Gool), pp. 103–120. North-Holland.
Stein, C. 1976 *Critical materials problems in energy production.* Academic Press.
Trasatti, S. (ed.) 1980 *Electrodes of conductive metallic oxides.* Elsevier.
Trumbore, F. A. 1979 *Pure appl. Chem.* **52**, 119–134.
von Alpen, U., Talat, G. H. & Rabenau, A. 1977 *Appl. Phys. Lett.* **30**, 621–623.
Whittingham, M. S. 1976 *Science, N.Y.* **192**, 1126–1127.
Whittingham, M. S. 1978 *Prog. Solid State Chem.* **12**, 41–99.
Winn, D. A., Shemilt, J. M. & Steele, B. C. H. 1976 *Mater. Res. Bull.* **11**, 559–566.

PHILOSOPHICAL TRANSACTIONS OF THE ROYAL SOCIETY A MATHEMATICAL, PHYSICAL & ENGINEERING SCIENCES

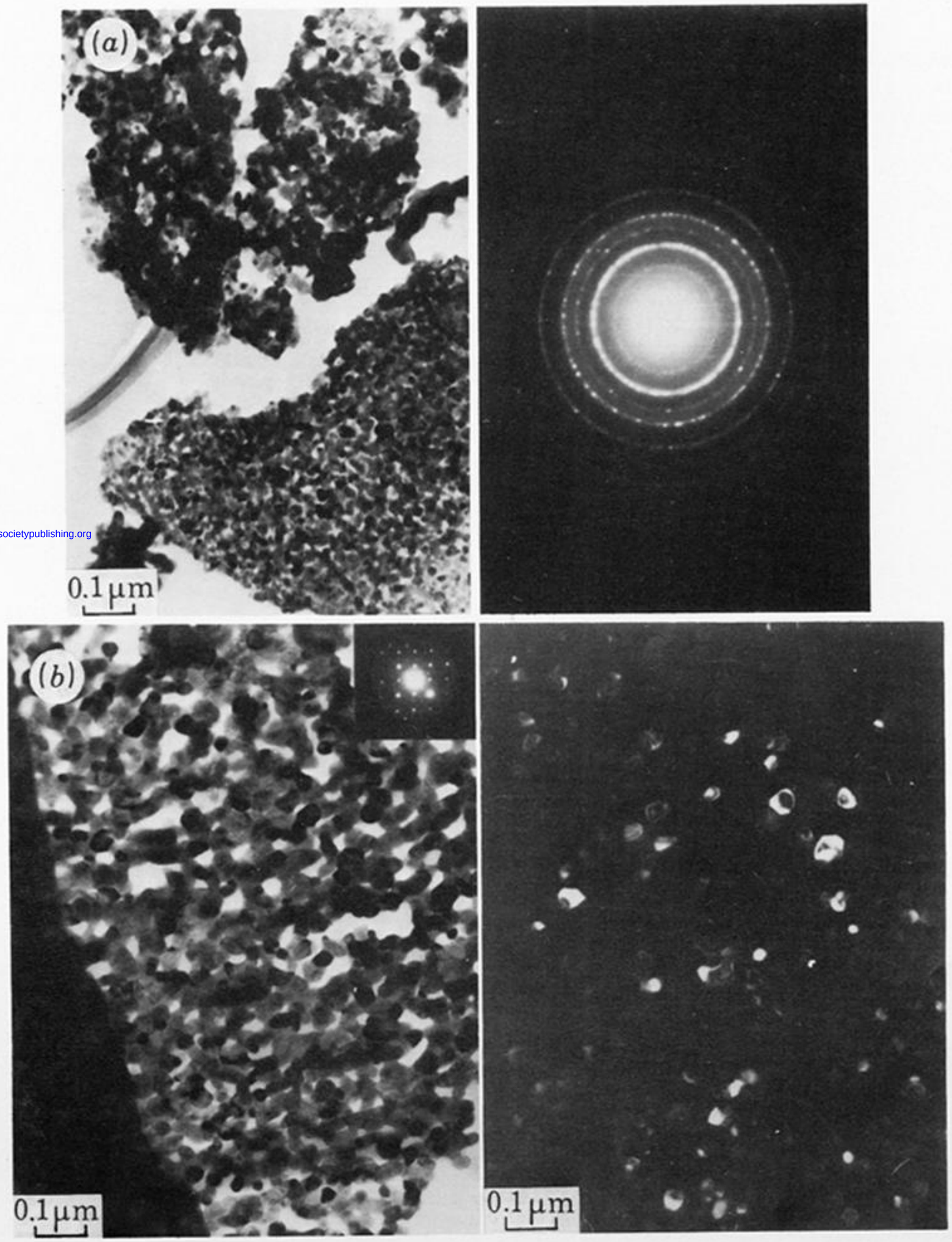

FIGURE 1. (*a*) Transmission electron micrograph of polycrystalline aggregate of $La_{0.7}Sr_{0.3}MnO_{3-x}$ electrocatalyst. The broad electron beam produces a polycrystalline ring diffraction pattern. (*b*) Transmission electron micrography (bright field image) of polycrystalline aggregate of $La_{0.7}Sr_{0.3}MnO_{3-x}$ electrocatalysts (left). Narrow electron beam enables single crystal diffraction spots to be obtained from small (*ca.* 50 nm) particles shown in dark field image (right).